Effector-Mediated Alteration of Substrate Orientation in Cytochrome P450 2C9†

Matthew A. Hummel,‡,|| Peter M. Gannett,‡ Jarrett S. Aguilar,§ and Timothy S. Tracy*,‡,||

Department of Basic Pharmaceutical Sciences, West Virginia University School of Pharmacy, Morgantown, West Virginia 26506, and Department of Natural Sciences and Mathematics, West Liberty State College, West Liberty, West Virginia 26074

Received December 1, 2003; Revised Manuscript Received April 8, 2004

ABSTRACT: Cytochrome P450 2C9 (CYP2C9)-mediated flurbiprofen 4′-hydroxylation is activated by the presence of dapsone resulting in reduction of the K_m for flurbiprofen hydroxylation and an increase in V_m. Previous spectral binding studies have demonstrated that the binding of flurbiprofen with CYP2C9 is increased (decrease in K_S) by the presence of dapsone. We hypothesized that the two compounds are simultaneously in the active site with the presence of dapsone causing flurbiprofen to be oriented more closely to the heme. T_1 relaxation rates determined by NMR were used to estimate the distances of protons on these compounds from the paramagnetic heme-iron center. Samples contained 0.014 μM CYP2C9 and 145 μM flurbiprofen in the presence and absence of 100 μM dapsone. Estimated distances of various flurbiprofen protons from the heme ranged from 4.2 to 4.5 Å in the absence of dapsone and from 3.2 to 3.8 Å in the presence of dapsone. The 4′ proton of flurbiprofen, the site of metabolism, showed one of the greatest differences in distance from the heme in the presence of dapsone, 3.50 Å, as compared to the absence of dapsone, 4.41 Å. Dapsone protons were less affected, being 4.40 Å from the heme in the absence of flurbiprofen and 4.00−4.01 Å from the heme in the presence of flurbiprofen. Molecular modeling studies were also performed to corroborate the relative orientations of flurbiprofen and dapsone in the active site of CYP2C9. Shift of the 4′ proton of flurbiprofen closer to the heme iron of CYP2C9 in the presence of dapsone may play a role in activation.

Observations of atypical kinetic phenomena in cytochrome P450-mediated reactions are becoming increasingly common (*1*). One of the most unexpected of these atypical profiles is that of enzyme activation or heterotropic positive cooperativity, which occurs when substrate metabolism is increased in the presence of an effector molecule. Typically, when a second compound is added that is also metabolized by the enzyme, inhibition of the object substrate compound is expected. However, with activation, the rate of metabolism is increased without a corresponding increase in enzyme concentration. An example of enzyme activation is the increase in flurbiprofen 4′-hydroxylation by cytochrome P450 2C9 (CYP2C9)[1] when co-incubated in the presence of dapsone (Figure 1) (*2*). Enzyme activation has also been demonstrated with CYP3A4 and a number of substrate and effector molecules (*3*−*6*). Previous work has shown that co-incubation with dapsone reduces uncoupling of the CYP2C9 catalytic cycle resulting in diminished water and hydrogen peroxide formation (*7*). This reduction in uncoupling results in a greater number of productive catalytic cycles and thus increased substrate turnover.

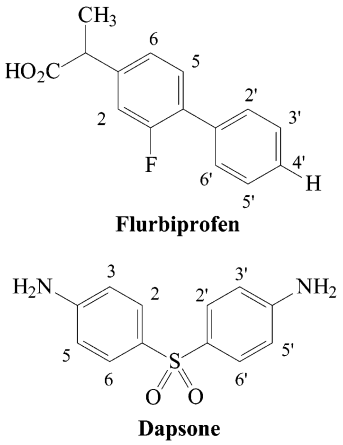

FIGURE 1: Structures of flurbiprofen and dapsone. Numbering schemes used in the text are shown.

It has been previously suggested that one causative factor in these atypical kinetic profiles, such as positive cooperativity, may be the binding of two molecules (in this case, molecules of two different compounds, i.e., heteroactivation) within the enzyme active site simultaneously. This hypothesis is supported by both kinetic data and spectral binding data. When dapsone is present in the incubation

† This work was supported in part by grants from the Public Health Service (Grant GM-63215 to T.S.T), National Center for Research Resources (Grant 1P20RR16477 to J.S.A.) and NSF (Grant 1002165R to P.M.G.).

* Corresponding Author. Mailing address: Department of Experimental and Clinical Pharmacology, College of Pharmacy, University of Minnesota, 7-168 Weaver-Densford Hall, 308 Harvard St. SE, Minneapolis, MN 55455. Tel: 612-625-7665. Fax: 612-625-3927. E-mail: tracy017@umn.edu.

‡ West Virginia University School of Pharmacy.

|| Current Address: Department of Experimental and Clinical Pharmacology, College of Pharmacy, University of Minnesota, Minneapolis, MN 55455.

§ West Liberty State College.

[1] Abbreviations: CYP2C9, cytochrome P450 2C9; V_m, maximal reaction velocity; K_m, Michaelis−Menten constant; K_s, Spectral binding constant; K_D, NMR-determined binding constant; T_1, T_1 relaxation time; τ_c, correlation time; α_m, relative mole fraction of total P450 to substrate.

10.1021/bi036158o CCC: $27.50
Published on Web 05/08/2004

mixture along with flurbiprofen and other NSAIDs, the resulting data can be fit with a two-site model that shows not only an increase in V_m but also a reduction in K_m (*2*, *8*). For example, for CYP2C9.1-mediated flurbiprofen 4′-hydroxylation, the V_m was increased ~1.7-fold and the K_m decreased ~3-fold in the presence of 100 μM dapsone in comparison to the absence of dapsone (*2*). Dapsone is also a CYP2C9 substrate, resulting in the production of *N*-hydroxydapsone, and this reaction has been shown to be unaffected by co-incubation with flurbiprofen (*2*). Interestingly, this metabolite of dapsone, *N*-hydroxydapsone, is also capable of activating CYP2C9-mediated metabolism (*7*). It has also been noted that dapsone increases the binding affinity of flurbiprofen with the CYP2C9 enzyme. Spectral binding studies have demonstrated that in the absence of dapsone, the binding constant (K_s) of flurbiprofen with CYP2C9 was 14 μM compared to 2 μM in the presence of dapsone, while *N*-hydroxydapsone had no effect on K_s (*7*). The recently published crystal structure of CYP2C9 shows adequate active site volume to accommodate multiple substrate molecules (*9*), lending further credence to the role of dual substrate binding in CYP2C9 activation. However, the exact mechanism for this increase in substrate turnover remains to be elucidated. One area for exploration is whether the presence of two molecules within the enzyme active site results in a change in position of the substrate molecule with respect to the heme oxygen of cytochrome P450. A change in substrate position such that the site of metabolism is located closer to the heme should result in an increase in substrate turnover (*10*).

Regal and Nelson have successfully used nuclear magnetic resonance (NMR)-derived T_1 relaxation times to assess the distance of substrate protons from the heme of cytochrome P450 (*11*). In the presence of paramagnetic molecules such as iron, the relaxation time is shortened in a distance-dependent manner (*11*, *12*). Since the heme of cytochrome P450 contains iron, the T_1 times of those substrate protons closest to the heme iron will show larger decreases than T_1 times of those farther away. In turn, the T_1 times can be used to calculate the relative distances between the protons of a substrate and the heme iron (*11*, *12*). This methodology has been applied to several cytochrome P450−substrate examples, including sodium laurate (CYPBM3), caffeine (CYP1A1), codeine (CYP2D6), and diclofenac (CYP2C9) (*11*, *13*−*15*), and is applicable to simultaneous substrate binding and activation of CYP2C9. It should be possible to determine not only flurbiprofen proton distances to the cytochrome P450 heme iron, but also those of the effector molecule, dapsone. Finally, we theorized that by measuring proton distances of each molecule interacting with cytochrome P450 alone and comparing them to an experiment in which both compounds, flurbiprofen and dapsone, were present with the enzyme, we could assess whether either compound affected the distances of the other relative to the heme and, particularly, whether protons at the site of metabolism were shifted (*11*).

MATERIALS AND METHODS

Materials. Potassium phosphate, glycerol, and EDTA were purchased from Fisher Scientific (Pittsburgh, PA). D_2O, poly(vinylpyrrolidone), dapsone, and sodium dithionite were obtained from Sigma-Aldrich (St. Louis, MO). Glycerol-d_8 was obtained from Cambridge Isotopes Laboratory (Andover, MA). (*S*)-Flurbiprofen was a gift from the Pharmacia Corporation (Kalamazoo, MI). Carbon monoxide was purchased from Mountain State AirGas (Morgantown, WV). Centricon MW cutoff filters were obtained from Millipore (Billerica, MA). NMR spectra were acquired on either a Varian Inova 500 (National High Field Magnet Laboratory, Tallahassee, FL) or a Varian Inova 600 MHz NMR (West Virginia University, Morgantown, WV) at 25 °C, unless otherwise noted.

Chemical Shift Assignments. Chemical shift assignments for flurbiprofen and dapsone protons (Figure 1) were made on the basis of correlation spectroscopy (COSY) and nuclear Overhauser effect (NOE) data (flurbiprofen) and chemical shifts (dapsone).

NMR Titration Experiments. Human cytochrome P450 2C9 was expressed and purified according to previously established methods (*16*). The purified CYP2C9 enzyme was concentrated to 50 μM in 1 mL using a Centricon 30K MW cutoff centrifugation filter prerinsed with 50 mM potassium phosphate buffer (pH 7.4) containing 20% glycerol-d_8, 1% poly(vinylpyrrolidone), and 1 mM EDTA in D_2O (*11*). The resulting sample was used to titrate a solution of flurbiprofen and dapsone (1:1, 50 μM each, 1 mL) in 50 mM potassium phosphate buffer (pH 7.4) containing 20% glycerol-d_8 and D_2O. The enzyme was added in 0.1 equiv increments, and spectra were recorded.

T_1 Relaxation Time Measurements. T_1 times of substrate protons were determined with the NMR operating at 599.7 MHz, internally locked on the deuterium signal of the solvent. The probe was maintained at 298 K for all experiments except for those involving temperature dependence. The Varian T_1 inversion−recovery sequence (d_1−180−d_2−90) was used along with presaturation of the residual HOD signal. The PW 90 was calibrated on each sample. Samples were prepared as for the titration experiments with a final concentration of 42 μM and then diluted 50-fold into 50 mM potassium phosphate (pH 7.4) in D_2O to remove the majority of the glycerol and H_2O. The enzyme was then added to the sample tube at a concentration of 0.014 μM in a final volume of 750 μL containing either 145 μM (*S*)-flurbiprofen, 145 μM (*S*)-flurbiprofen and 100 μM dapsone, or 100 μM dapsone alone. Spectra were acquired for 12 τ (d_2) values ranging from 0.0125 to 25.6 s and a period of 10 T_1 was used between pulses (d_1). The Varian software routines were used to determine the T_1 times. Once the paramagnetic effect of the heme iron on substrate protons was measured, CO was bubbled through the sample for 15 min, and sodium dithionite was added and allowed to equilibrate for 30 min to determine the diamagnetic contribution to the T_1 relaxation times. Stability of the enzyme as well as the CO reduced complex was tested and found to be stable for the duration of the NMR acquisition time.

T_1 Relaxation Time Temperature Dependence. The validity of the T_1 measurements and the distances calculated between protons in flurbiprofen and dapsone is dependent on the substrates being in fast exchange. This can be demonstrated by conducting T_1 measurements over a range of temperatures (*11*). Therefore, T_1 measurements were performed as described above at three different temperatures (283, 298, and 310 K). Data were collected both in the absence ($1/T_{1,2C9}$) and presence ($1/T_{1,2C9+CO}$) of CO/sodium dithionite. To

ensure adequate diffusion of CO and mixing of dithionite, samples were removed from the NMR tube and placed in a test tube, CO was bubbled, and sodium dithionite was added, and then the sample was placed back into the NMR tube. Plots of $1/T_{1,2C9}$, $1/T_{1,2C9+CO}$, and $1/T_{1p}$ (equal to $1/T_{1,2C9}$ minus $1/T_{1,2C9+CO}$) versus 1/temperature were positive in all cases.

Distance Calculation. Estimates for distances of protons from the heme iron of CYP2C9 were calculated using the following equation: $r = C[T_{1p}\alpha_m f(\tau_c)]^{1/6}$, where r is the distance and C is a constant that is a function of the metal, oxidation state, and whether it is low or high spin. In this case, Fe^{3+} is in the low-spin state, and thus the appropriate value for C is 539 (*12*). T_{1p} is the portion of T_{1obs} due to paramagnetic affects alone and is given by $T_{1p}^{-1} = T_{1obs}(Fe^{3+})^{-1} - T_{1obs}(Fe^{2+})^{-1}$ assuming that all of the diamagnetic contribution is represented by $T_{1obs}(Fe^{2+})$ (*11*). This assumption has been used in many similar studies and appears to be generally valid (*14*, *15*, *17*). The parameter α_m is equal to [P450]/(K_S + [substrate]) under conditions of fast exchange (*11*). The distance calculations require values for K_D for the substrates and τ_c of the enzyme. We have used the flurbiprofen K_S (14 μM in the absence of dapsone, 2.0 μM in the presence of dapsone) determined from visible spectroscopy rather than K_D determined by NMR for flurbiprofen. Ideally, K_D (determined by NMR) would be used in place of K_S (determined by UV/vis). For a process behaving according to Michaelis−Menten kinetics (which flurbiprofen 4′-hydroxylation does), K_S and K_D should be similar if not equal and any difference between them should be small. A K_S for dapsone could not be determined, and we have used K_m (100 μM) instead. However, the extent to which K_m does not equal K_D will only affect distances calculated for dapsone. The correlation time (τ_c) for CYP2C9 has been previously reported (2×10^{-10} s^{-1}) (*15*) and was used here.

Molecular Modeling. The structures for flurbiprofen and dapsone were generated using the Builder module of the InSight 2000 (Accelrys, San Diego, CA) software package. The structures were then minimized using the Builder Optimize protocol with the default settings. The CYP2C9 structure was obtained from Dr. Jeffrey P. Jones (http://joneslab.wsu.edu/homology.htm). This CYP2C9 structure is a homology model based on the crystal structure of mammalian P450 2C5. The protein was then edited in the Biopolymer module of the Insight 2000. The heme cofactor was removed and replaced with the oxoheme cofactor and parametrized (*18*, *19*). Molecular dynamics and minimization were then carried out on the modified CYP2C9 using a nonbonded cutoff of 15 Å in the Discover module. A 1000 step minimization using steepest descents was followed by 10 000 steps (1 fs time step) of molecular dynamics and then another 1000 step minimization. All other parameters were set at their default values. The resulting structure was used for subsequent docking studies.

Docking of flurbiprofen into the model was done using the Affinity module of the software. The substrate structure was placed into the active site of the CYP2C9, and the docking parameters were set to their default values with two exceptions. First, the simulated annealing was applied using default parameters for the annealing step, and second, final minimization is turned on. The same procedure was used to dock the dapsone structure into the active site of the protein.

Table 1: Chemical Shift Assignments for Flurbiprofen[a]

proton	chemical shift (ppm)	multiplicity[b]	coupling constant (Hz)
CH_3	1.43	d	7.2
CH	3.66	q	7.2
H-2	7.03	dd	1.2, 11.5[c]
H-5	7.32	dd	1.2, 7.8
H-6	7.06	d	7.8
H-2′/6′	7.46	dd	1.2, 8.1
H-3′/5′	7.35	t	8.1
H-4′	7.27	tt	1.2, 8.1

[a] Spectra were recorded in D_2O at 25 °C, and reported shifts are referenced to 3-(trimethylsilyl)propane-1-sulfonic acid. [b] d = doublet; dd = doublet of doublets; q = quartet; t = triplet; tt = triplet of triplets. [c] The 11.5 Hz coupling is for J_{H-F} between H-2 and F-3.

Table 2: Chemical Shift Assignments for Dapsone[a]

proton	chemical shift (ppm)	multiplicity[b]	coupling constant (Hz)
H-2/2′/6/6′	7.60	d	8.5
H-3/3′/5/5′	6.76	d	8.5

[a] Spectra were recorded in D_2O at 25 °C, and reported shifts are referenced to 3-(trimethylsilyl)propane-1-sulfonic acid. [b] d = doublet.

For docking two substrates at once, one conformation of the docked flurbiprofen was merged with the protein such that it becomes the target and then dapsone was docked with the enzyme−flubiprofen complex. The docking parameters were the same as those for running the single substrate docking procedure with flurbiprofen or dapsone alone. The same procedure was carried out merging dapsone and the protein and docking flurbiprofen into the target. A total of 20 lowest energy orientations of flurbiprofen, dapsone, or flurbiprofen/dapsone were identified. The lowest 10 were then subjected to simulated annealing.

RESULTS

The chemical shifts, coupling constants, and peak multiplicities for flurbiprofen are presented in Table 1, and those for dapsone are presented in Table 2. Initially, an isotope-edited experiment (*20*) was attempted using dapsone-d_8 (*21*) to demonstrate that both flurbiprofen and dapsone were in the active site of CYP2C9 simultaneously. The ^1H NMR spectra of CYP2C9 were unsatisfactory for this experiment due to extensive line broadening displayed by the sample, likely due to slow tumbling of the CYP2C9. However, the line broadening did suggest that both flurbiprofen and dapsone simultaneously bind to the enzyme. Thus, when a sample containing a 1:1 mixture of flurbiprofen and dapsone was titrated with CYP2C9 enzyme, the resonances of both flurbiprofen and dapsone broadened (Figure 2). This is the expected result if both flurbiprofen and dapsone bind to the enzyme because when they bind they take on the slow tumbling characteristics of the enzyme in the NMR sample. The result does not conclusively prove that both substrates were simultaneously in the active site, and thus, T_1 studies were undertaken to demonstrate simultaneous binding.

T_1 measurements were undertaken, and it was observed that distance-dependent decreases in T_1 relaxation times of protons of bound substrates in the presence of the iron-containing CYP2C9 enzyme were noted relative to the T_1 relaxation times of the same protons in the same sample

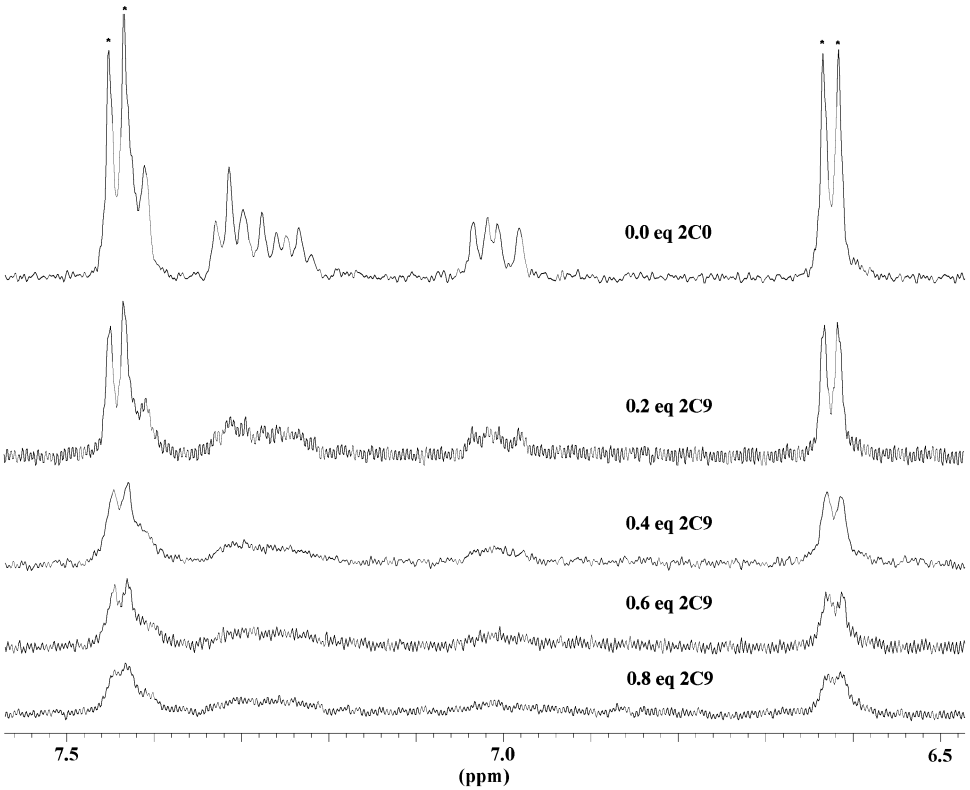

FIGURE 2: NMR spectra of the titration of a 1:1 mixture of flurbiprofen and dapsone with CYP2C9. Samples, from the top, contained 0.0 equiv, 0.2 equiv, 0.4 equiv, 0.6 equiv, and 0.8 equiv of CYP2C9. Only the aromatic region is shown. Peaks marked with ∗ are due to dapsone, and unmarked peaks are due to flurbiprofen.

Table 3: T_1 and Calculated Distances of Flurbiprofen and Dapsone in the Active Site of Cytochrome P450 2C9[a]

proton resonance[c]	flurbiprofen or dapsone				flurbiprofen and dapsone			
	2C9[d]	2C9 + CO	r[e]	r[f]	2C9[g]	2C9 + CO	r[e]	r[f]
				Flurbiprofen[b]				
CH_3	0.69(0.01)	0.72(0.01)	4.39(0.14)	6.96	0.63(0.02)	0.72(0.02)	3.16(0.10)	6.21
H-2	2.28(0.15)	2.59(0.21)	4.49(0.35)	5.95	2.13(0.15)	2.50(0.16)	3.76(0.26)	5.44
H-5	1.86(0.12)	2.14(0.13)	4.28(0.28)	5.93	1.71(0.20)	2.22(0.18)	3.37(0.40)	5.71
H-6	1.71(0.09)	1.98(0.04)	4.19(0.22)	5.39	1.63(0.09)	1.83(0.1)	3.79(0.20)	5.18
H-2′/6′	2.26(0.08)	2.61(0.02)	4.40(0.15)	5.04	2.14(0.07)	2.62(0.09)	3.64(0.33)	5.00
H-3′/5′	2.27(0.10)	2.59(0.11)	4.47(0.20)	5.87	2.16(0.10)	2.72(0.18)	3.57(0.23)	5.51
H-4′	3.00(0.27)	3.50(0.34)	4.41(0.44)	6.3	2.57(0.26)	3.54(0.39)	3.50(0.39)	5.79
				Dapsone[b]				
H-2/2′/6/6′	3.41(0.11)	4.61(0.25)	4.40(0.23)	5.27	3.58(0.11)	4.31(0.11)	4.01(0.12)	6.86
H-3/3′/5/5′	3.61(0.12)	5.14(0.20)	4.40(0.17)	5.12	3.95(0.15)	4.88(0.11)	4.00(0.15)	5.36

[a] Errors for measurements are shown in parentheses. Errors in the T_1 values were those reported by the fitting routine. Errors in the reported distances (r) were determined by propagation of error from the T_1 calculation. Generally, the error is <10%. [b] [Flurbiprofen] = 145 μM; [dapsone] = 100 μM. [c] See Figure 1 for numbering scheme of the protons for flurbiprofen and dapsone. T_1 times for the HC−CO_2H proton could not be accurately determined due to interference from the residual glycerol resonances. [d] T_1 values are in seconds. [CYP2C9] = 0.014 μM; α_m = [P450]/(K_S + [substrate]), K_S(flurbiprofen) = 14.0 μM (*7*); α_m(flurbiprofen) = 8.81 × 10^{-5}; K_S(dapsone) = 100 μM (not obtainable by UV spectroscopy, assumed $K_S = K_m$) (*2*); α_m(dapsone) = 7.0 × 10^{-5}. [e] Values are in angstroms (Å); $r = C[T_{1p}\alpha_m f(\tau_c)]^{-1/6}$; C = 539 (*12*); $1/T_{1p} = 1/T_{1,2C9} - 1/T_{1,2C9+CO}$ (*12*); $f(\tau_c) = 2 \times 10^{-10}$ s^{-1}. [f] Values were obtained by averaging the 20 lowest-energy conformations obtained from molecular dynamics. [g] T_1 values are in seconds. K_S(flurbiprofen) = 2.0 μM; K_S(dapsone) = 100 μM (not obtainable by UV spectroscopy, assumed $K_S = K_M$) (*2*); α_m = 4.03 × 10^{-5}.

treated with carbon monoxide. T_1 relaxation times for protons of flurbiprofen, dapsone, and a mixture of flurbiprofen and dapsone in the presence of CYP2C9 without and with carbon monoxide are shown in Table 3.

Inspection of the data reveal that T_1 relaxation times are decreased for all protons of flurbiprofen or dapsone in the presence of CYP2C9 relative to those times measured in the presence of CYP2C9 and carbon monoxide. The differences in T_1 relaxation times also permit calculation of the distance between flurbiprofen or dapsone and the heme iron (Table 3). There is a substantial difference in T_1 relaxation times between the samples with and without carbon monoxide. For this to be observed requires the substrates to be binding to the active site. Representative spectra for samples containing CYP2C9 and flurbiprofen in the presence and absence of carbon monoxide are shown in Figure 3A,B (flurbiprofen H-3′/5′, H-4′, and H-5 only). The difference in T_1 relaxation times between samples without and with carbon monoxide can be clearly seen as the resonances go through a null (decreased T_1) earlier in the presence of CYP2C9 enzyme alone as compared to in the presence of carbon monoxide bound CYP2C9.

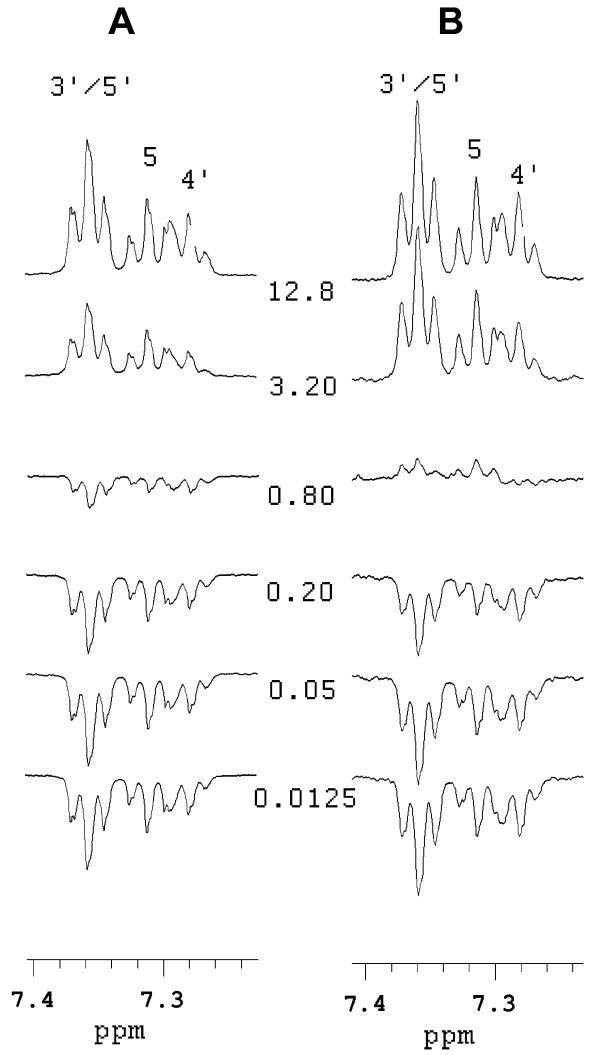

FIGURE 3: T_1 relaxation data for (A) flurbiprofen/CYP2C9/carbon monoxide and (B) flurbiprofen/CYP2C9. The delay times (s) for each spectrum are shown in the center. These data were obtained with a two-pulse (with HOD presaturation) experiment. The first was a 180° pulse to invert the magnetization, a variable delay was then inserted, and then a second, 90° observed pulse was used. A delay between each acquisition of 30 s was used (greater than 10 T_1's). The resonances for the 3′-, 4′-, 5′-, and 5-protons of flurbiprofen, only, are shown (refer to Figure 1 for structures and numbering scheme). It can be seen that these resonances go through a null (decreased T_1) earlier in the presence of CYP2C9 (ca. 0.8 s) than in the presence of CYP2C9/carbon monoxide (ca. 1.3 s).

The validity of the distances derived from T_1 relaxation times of substrate protons requires the system to be operating under fast-exchange conditions, meaning that substrate molecules in the active site must be rapidly exchanging with those in bulk solution. The temperature dependence of the T_1 relaxation of the substrate protons is used to verify fast-exchange conditions (*11*). A positive slope in the double reciprocal plot of T_{1p} versus temperature indicates that the fast exchange condition is being met. This condition also requires that double reciprocal plots of $T_{1,2C9}$ or $T_{1,2C9+CO}$ versus temperature be of a positive slope. The double reciprocal plots of T_{1p} and $T_{1,2C9}$ versus temperature are shown in Figure 4 and support the claim that the fast exchange requirement has been satisfied. A similar plot was obtained from the double reciprocal plot of $T_{1,2C9+CO}$ (data not shown).

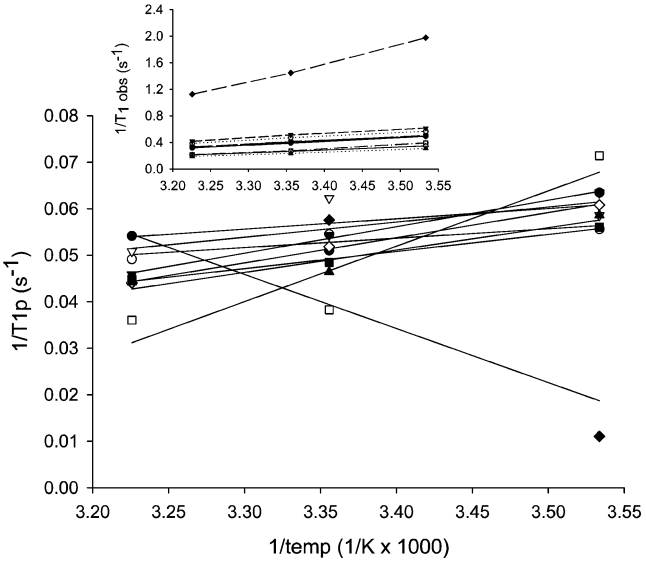

FIGURE 4: Temperature dependence of T_{1p} times for flurbiprofen and dapsone. A positive linear slope is indicative of fast-exchange conditions. The inset shows a plot of T_{1obs} vs 1/temp. Protons are represented as follows: flurbiprofen H-2 (●), H-5 (○), H-6 (▼), H-2′/6′ (▽), H-3′/5′ (■), H-4′ (□), CH_3 (◆); dapsone H-2/2′/6/6′ (◇), H-3/3′/5/5′ (▲). One data point (flurbiprofen methyl proton observed at a temperature of 283 K) was higher (thus inverse value was lower) than other two data points (lower temperatures) causing the slope of this line to be negative. However, since the slopes of the lines for 6 of the 7 monitored flurbiprofen protons are positive and, therefore, exhibiting fast-exchange conditions, it is assumed that all of these protons must be undergoing fast exchange with the bulk solution.

Preliminary molecular modeling studies have been conducted and aid in understanding the T_1 relaxation data reported in Table 3. In particular, when flurbiprofen was docked and annealed to the active site, the two lowest energy orientations for flurbiprofen were with the methyl group and with H-4′ near the heme (Figure 5). These structures differ by less than 2 kcal/mol. The orientation shown in Figure 5A (methyl group closest to the heme) is the slightly more stable orientation. This agrees with the proposal that the T_1 times, and hence the distances reported in Table 3 for protons on flurbiprofen, represent an average of the possible orientations flurbiprofen may adopt with respect to the heme. For comparison, also presented in Table 3 are the distances obtained by averaging the 20 lowest conformations of flurbiprofen. The calculated distances place flurbiprofen further away from the heme than the T_1 data, though there is a rough correlation between them. The largest differences occur at the ends of flurbiprofen (methyl and H-4′) suggesting that the model does not permit a sufficient range of motion.

When dapsone was docked and annealed, the lowest-energy structure that was obtained resulted in the average distance of the 3/3′/5/5′ protons (5.12 Å) being nearer to the heme than the 2/2′/6/6′ protons (5.27 Å). As with flurbiprofen, there is a rough correlation between the calculated and T_1-derived distances, and the calculated distances were overestimated. Finally, when both flurbiprofen and dapsone were docked in the active site and annealed, the structure shown in Figure 6 was obtained. This structure places H-4′ nearer the heme (5.79 Å) than in the absence of dapsone (6.3 Å). Dapsone, relative to the structure obtained in the absence of flurbiprofen, has been displaced from the

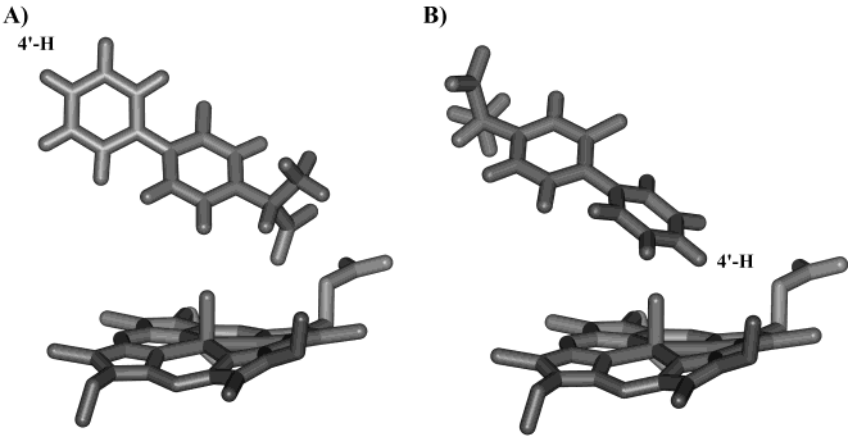

FIGURE 5: The two lowest-energy structures of flurbiprofen docked in the active site of CYP2C9 with either (A) the methyl group end or (B) the H-4′ end of flurbiprofen nearest the heme iron. In either case, the 4′-H is indicated.

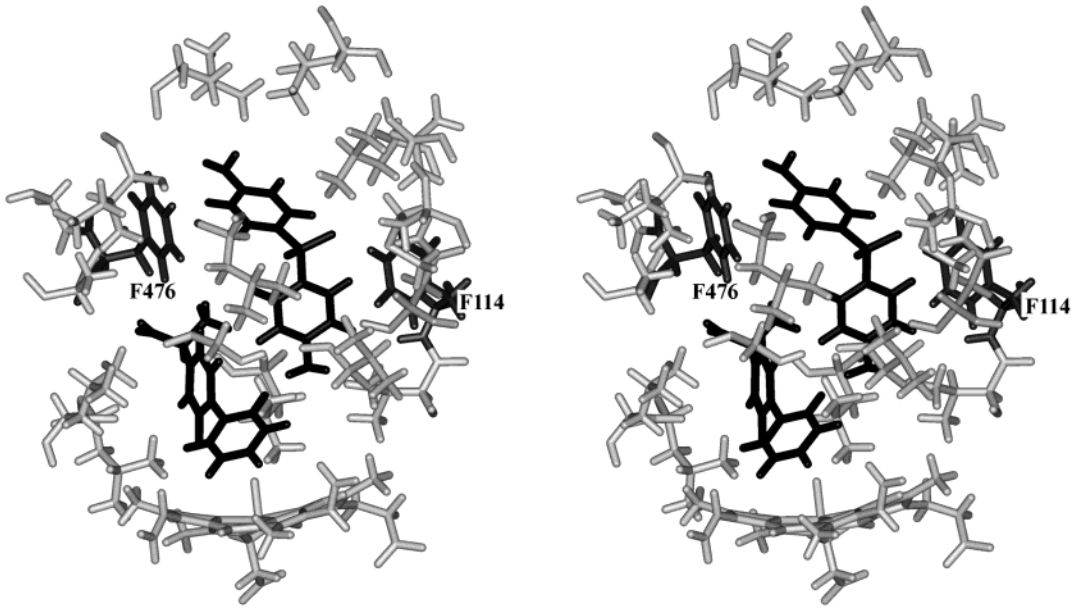

FIGURE 6: Stereoview of flurbiprofen and dapsone in the active site of CYP2C9. Flurbiprofen (center) and dapsone are in black and residues Phe476 (F476 left) and Phe114 (F114, right) in dark gray. Flurbiprofen occupies region A, (*9*) extending into the middle region, and dapsone is completely within the middle region of the active site. Region B is unoccupied.

heme as reflected in the calculated distances for both the 3/3′/5/5′ and 2/2′/6/6′ protons, in agreement with the trends calculated from the T_1 data. Note that the models shown in Figures 5 and 6 are useful for interpreting the T_1 data and provide a rationale for why similar distances are obtained for protons on opposite ends of flurbiprofen. Differences between the calculated and experimental values are, in part, because the distances calculated from the models are based on a very small subset of orientations, while the distances calculated from the T_1 data represent a large number of possible orientations. A more accurate picture of the probable arrangement of flurbiprofen, dapsone, and the combination of flurbiprofen/dapsone will require molecular dynamics computations.

DISCUSSION

Kinetic and spectral binding data regarding the activation of CYP2C9-mediated flurbiprofen metabolism by dapsone suggest that this phenomenon was due, at least in part, to both compounds (flurbiprofen and dapsone) being present within the active site simultaneously. However, concrete evidence to this effect has been lacking. From NMR titration and T_1 relaxation time measurements, the current data provide evidence that dapsone and flurbiprofen are simultaneously occupying the active-site cavity of CYP2C9 and that the concurrent presence of dapsone causes the flurbiprofen molecule, specifically the site of metabolism, to be oriented closer to the heme iron of the enzyme. These findings were then corroborated with computer modeling studies of both flurbiprofen and dapsone orientation within the active site of CYP2C9.

The titration experiment, showing the resonances of flurbiprofen and dapsone broadening, suggests that the substrates were binding simultaneously to the enzyme since the resonances of both flurbiprofen and dapsone broadened in the presence of enzyme (Figure 2). However, this experiment does not permit determination of the exact site of flurbiprofen and dapsone binding because (1) both flurbiprofen and dapsone could be in the active site, (2) one of the two could be bound to the active site while the second could be bound, for example, on the surface of the enzyme, or (3) both could be bound at locations other than the active

site. Consequently, attention was shifted to T_1 measurements, which allow assessment of proton distances from the heme iron. Those substrate protons nearest the paramagnetic heme iron (Fe^{3+}) of CYP2C9 enzyme will show the greatest decrease in T_1 relaxation times. Additionally, these effects will be greater than those in an enzyme preparation where the iron has been bound with carbon monoxide and reduced with sodium dithionite, causing the heme iron to become Fe^{2+}, thereby controlling for any diamagnetic contribution of the protein to the T_1 relaxation times of substrate protons (*11*). Therefore, T_1 measurements allow determination of whether a substrate binds to the active site of CYP2C9 and, if it binds, its average orientation in the active site (*12*).

The data for flurbiprofen initially appear somewhat contradictory because the calculated distance between the heme iron and the methyl group is 4.39 Å and that between the heme iron and H-4′ is 4.41 Å. These separations are not possible if flurbiprofen only binds in one orientation. Consequently, these findings suggest that two binding orientations are adopted by flurbiprofen, one in which the methyl group is near the heme and a second in which the H-4′ end binds near the heme. If this is the case, then the distances reported in Table 3 for flurbiprofen represent the average of these two orientations. Note that dapsone may also adopt more than one orientation with respect to the heme but due to the symmetry of dapsone, this cannot be determined. However, the distances observed for dapsone, in the absence of flurbiprofen, are consistent with the known metabolism of dapsone, which is conversion of the NH_2 group to −NHOH. Thus, it would be predicted that the heme would be nearer to the 3/3′/5/5′ protons than to the 2/2′/6/6′ protons as observed, though this depends on the specifics of the orientation of dapsone relative to the heme in the active site.

The data shown in Table 3 for samples containing both flurbiprofen and dapsone show that the T_1 relaxation times of the flurbiprofen protons are all decreased (except H-6), relative to those samples that do not contain dapsone. Also, the distances calculated from the heme to H-3/3′/5/5′ of dapsone are greater than they are in the absence of flurbiprofen. These results suggest that dapsone forces flurbiprofen nearer the heme iron, and because of this, dapsone must move away from the active site. The data also show that, on average, the 2/2′/6/6′ protons of dapsone are nearer the heme in the presence of flurbiprofen than in its absence, suggesting that the dapsone molecule adopts a different orientation in the active site relative to samples that did not contain flurbiprofen.

Most importantly, the data demonstrate that when both flurbiprofen and dapsone are present, both must occupy the active site simultaneously. If only one substrate was occupying the active site in the samples containing both dapsone and flurbiprofen, the T_1 relaxation times would be identical to those samples containing either flurbiprofen or dapsone alone. However, in samples containing both, the T_1 times of both flurbiprofen and dapsone are altered relative to when either substrate is present alone. The observed changes in T_1 relaxation times, which show that flurbiprofen moves nearer the heme in the presence of dapsone, correlate with previously reported metabolism data because flurbiprofen is metabolized at the 4′-position and the rate of flurbiprofen metabolism is increased in the presence of dapsone (*2*, *8*). These findings of simultaneous substrate occupation also corroborate data from the recently reported crystal structure of human CYP2C9 because it has been reported that the active site of this enzyme is sufficiently large to accommodate two substrates simultaneously (*9*). During the course of our studies, a preliminary report was presented in abstract form demonstrating interactions within the CYP3A4 active site (*22*). This report described the alteration in the drug midazolam by the chemical α-naphthoflavone, causing midazolam metabolism sites to become closer to the heme iron. Though involving different compounds and another P450 enzyme, this study corroborates our results.

By conducting T_1 NMR studies, we have demonstrated that flurbiprofen and dapsone can bind simultaneously to the CYP2C9 active site. Furthermore, concurrent binding by dapsone causes the flurbiprofen substrate molecule to become more closely oriented to the heme iron such that it is more amenable to undergoing oxidation. This alteration of flurbiprofen orientation as a result of dapsone binding is most pronounced at the H-4′ proton, which is the primary site of oxidation. These findings correlate well with previously published results demonstrating that co-incubation of dapsone with flurbiprofen and CYP2C9 results not only in an increase in flurbiprofen turnover (activation) (*2*) but also in an increased flurbiprofen binding affinity (K_s) and a decrease in enzyme uncoupling (*7*). That the flurbiprofen site of metabolism moves closer to the heme iron helps explain the substantial decrease in K_m and increase in V_m for the production of 4′-hydroxyflurbiprofen noted when the two compounds are co-incubated (*2*). Furthermore, it would seem plausible that this closer proximity to the heme would result in more efficient coupling of the P450 reaction cycle and thus less resulting nonproductive water and peroxide formation, as has been previously observed during dapsone and flurbiprofen co-incubation (*7*). By performing stoichiometric measurements of camphor and ethylbenzene metabolism by P450cam and site-directed mutants, Loida and Sligar have previously demonstrated that a reduction in active-site volume and subsequent decreased substrate mobility within the active site caused a decrease in uncoupling of the P450 reaction cycle resulting in more efficient product formation with less water and hydrogen peroxide formation (*10*). It remains to be discovered whether this change in flurbiprofen orientation is caused by dapsone simply occupying space within the active site such that the movement of flurbiprofen molecules is hindered or whether the binding of dapsone to the CYP2C9 active site causes a conformational change in the enzyme such that the site available for flurbiprofen binding is physically altered. In this regard, Sibbesen et al. demonstrated that addition of more bulky substituents (presumably reducing molecule movement within the active site) to a series of alkylbenzenes resulted in an increase in coupled turnover by P450cam (*23*). Conversely, Schulze et al. reported that different conformational changes in P450cam were effected by the binding of the (1*S*)- and (1*R*)-enantiomers of camphor suggesting that substituent binding can induce a conformational change that can be compound-dependent (*24*). Currently, studies are being conducted to address these questions as they relate to the activation of CYP2C9 by dapsone.

In summary, these data demonstrate that both flurbiprofen and dapsone can occupy the active site of CYP2C9 simul-

taneously. Furthermore, the presence of dapsone within the active site alters the orientation of flurbiprofen such that the site of metabolism becomes oriented more closely to the heme iron of the enzyme. This change in substrate orientation and proximity to the heme iron of P450 caused by concurrently present effector molecules most likely plays a role in the increased enzyme catalytic efficiency and increased substrate metabolism observed during heterotropic cooperativity.

ACKNOWLEDGMENT

We thank the National High Field Magnet Laboratory for the use of the NMR facilities (500 MHz).

REFERENCES

1. Hutzler, J. M., and Tracy, T. S. (2002) Atypical kinetic profiles in drug metabolism reactions, *Drug Metab. Dispos. 30*, 355−362.
2. Hutzler, J. M., Hauer, M. J., and Tracy, T. S. (2001) Dapsone activation of CYP2C9-mediated metabolism: evidence for activation of multiple substrates and a two-site model, *Drug Metab. Dispos. 29*, 1029−1034.
3. Shou, M., Grogan, J., Mancewicz, J. A., Krausz, K. W., Gonzalez, F. J., Gelboin, H. V., and Korzekwa, K. R. (1994) Activation of CYP3A4: Evidence for the simultaneous binding of two substrates in a cytochrome P450 active site, *Biochemistry 33*, 6450−6455.
4. Kenworthy, K. E., Clarke, S. E., Andrews, J., and Houston, J. B. (2001) Multisite Kinetic Models for CYP3A4: Simultaneous Activation and Inhibition of Diazepam and Testosterone Metabolism, *Drug Metab. Dispos. 29*, 1644−1651.
5. Galetin, A., Clarke, S. E., and Houston, J. B. (2002) Quinidine and haloperidol as modifiers of CYP3A4 activity: multisite kinetic model approach, *Drug Metab. Dispos. 30*, 1512−1522.
6. Nakamura, H., Nakasa, H., Ishii, I., Ariyoshi, N., Igarashi, T., Ohmori, S., and Kitada, M. (2002) Effects of endogenous steroids on CYP3A4-mediated drug metabolism by human liver microsomes, *Drug Metab. Dispos. 30*, 534−540.
7. Hutzler, J. M., Wienkers, L. C., Wahlstrom, J. L., Carlson, T. J., and Tracy, T. S. (2003) Activation of cytochrome P450 2C9-mediated metabolism: mechanistic evidence in support of kinetic observations, *Arch. Biochem. Biophys. 410*, 16−24.
8. Korzekwa, K. R., Krishnamachary, N., Shou, M., Ogai, A., Parise, R. A., Rettie, A. E., Gonzalez, F. J., and Tracy, T. S. (1998) Evaluation of atypical cytochrome P450 kinetics with two-substrate models: Evidence that multiple substrates can simultaneously bind to cytochrome P450 active sites, *Biochemistry 37*, 4137−4147.
9. Williams, P. A., Cosme, J., Ward, A., Angove, H. C., Matak, V. D., and Jhoti, H. (2003) Crystal structure of human cytochrome P450 2C9 with bound warfarin, *Nature 424*, 464−468.
10. Loida, P. J., and Sligar, S. G. (1993) Molecular recognition in cytochrome P-450: mechanism for the control of uncoupling reactions, *Biochemistry 32*, 11530−11538.
11. Regal, K. A., and Nelson, S. D. (2000) Orientation of caffeine within the active site of human cytochrome P450 1A2 based on NMR longitudinal (T_1) relaxation measurements, *Arch. Biochem. Biophys. 384*, 47−58.
12. Mildvan, A. S., and Gupta, R. K. (1978) Nuclear relaxation measurements of the geometry of enzyme-bound substrates and analogs, *Methods Enzymol. 49*, 322−359.
13. Modi, S., Primrose, W. U., Boyle, J. M., Gibson, C. F., Lian, L. Y., and Roberts, G. C. (1995) NMR studies of substrate binding to cytochrome P450 BM3: comparisons to cytochrome P450 cam, *Biochemistry 34*, 8982−8988.
14. Modi, S., Paine, M. J., Sutcliffe, M. J., Lian, L. Y., Primrose, W. U., Wolf, C. R., and Roberts, G. C. (1996) A model for human cytochrome P450 2D6 based on homology modeling and NMR studies of substrate binding, *Biochemistry 35*, 4540−4550.
15. Poli-Scaife, S., Attias, R., Dansette, P. M., and Mansuy, D. (1997) The substrate binding site of human liver cytochrome p450 2C9: An NMR study, *Biochemistry 36*, 12672−12682.
16. Haining, R. L., Hunter, A. P., Veronese, M. E., Trager, W. F., and Rettie, A. E. (1996) Allelic variants of human cytochrome P450 2C9: Baculovirus-mediated expression, purification, structural characterization, substrate stereoselectivity, and prochiral selectivity of the wild-type and I359L mutant forms, *Arch. Biochem. Biophys. 333*, 447−458.
17. Shafirovich, V., Mock, S., Kolbanovskiy, A., and Geacintov, N. E. (2002) Photochemically catalyzed generation of site-specific 8-nitroguanine adducts in DNA by the reaction of long-lived neutral guanine radicals with nitrogen dioxide, *Chem. Res. Toxicol. 15*, 591−597.
18. Paulsen, M. D., and Ornstein, R. L. (1991) A 175-psec molecular dynamics simulation of camphor-bound cytochrome P-450cam13, *Proteins 11*, 184−204.
19. Paulsen, M. D., and Ornstein, R. L. (1992) Predicting the product specificity and coupling of cytochrome P450cam9, *J. Comput.-Aided Mol. Des. 6*, 449−460.
20. Fesik, S. W., and Zuiderweg, E. R. P. (1989) An approach for studying the active site of enzyme/inhibitor complexes using deuterated ligands and 2D NOE difference spectroscopy, *J. Am. Chem. Soc. 111*, 5013−5015.
21. Gannett, P. M., Johnson, E. M., Grimes, M. A., Myers, A. L., Deavers, R. E., and Tracy, T. S. (2003) Synthesis of deuterated 4,4′-diaminodiphenyl sulfone (Dapsone) and related analogues, *J. Labelled Compd. Radiopharm. 46*, 107−114.
22. Cameron, M. D., Allen, K. E., Wen, B., Campbell, A. P., and Nelson, S. D. (2003) NMR evidence for simultaneous binding of midazolam with alpha-naphthoflavone or testosterone with the active site of CYP3A4, Presented at Society of Toxicology 2003 Annual Meeting, Paper 335.
23. Sibbesen, O., Zhang, Z., and Ortiz de Montellano, P. R. (1998) Cytochrome P450cam substrate specificity: relationship between structure and catalytic oxidation of alkylbenzenes, *Arch. Biochem. Biophys. 353*, 285−296.
24. Schulze, H., Hoa, G. H., Helms, V., Wade, R. C., and Jung, C. (1996) Structural changes in cytochrome P-450cam effected by the binding of the enantiomers (1*R*)-camphor and (1*S*)-camphor, *Biochemistry 35*, 14127−14138.

BI036158O